Development of static P-Y curves from experimental measurements based on lateral load tests on onshore drilled shafts

Minh D. Uong[1] and J. Erik Loehr[2]

Abstract

Lateral load tests were performed at two geotechnical research sites. Drilled shafts were instrumented using both strain gages and shape acceleration array devices. Lateral deflection and bending moment profiles were interpreted from strain gages data as well as shape acceleration array data. p-y models were derived from the collected data using a Finite Element Method (FEM) code to match the measured experimental data. Linear and non-linear bending stiffness methodologies were used to develop the p-y curves. These analyses show that significantly different interpretations result when the non-linear bending stiffness is accurately modeled. A computational tool using FEM to incorporate non-linear bending stiffness is described along with analyses performed to compare the predicted lateral deflection and bending moment with experimental results. The evaluation described in this paper indicates the difference between the predicted p-y curves considering cracking and non-cracking concrete sections, as well as significant differences in lateral deflection and bending moment when non-linear bending stiffness is considered.

Key words: lateral load test, p-y curve, FEM, non-linear bending stiffness

(1) Ph.D., Faculty of Civil Engineering, Hanoi Architectural University
Geotechnical Engineer, Burns & McDonnell Engineering Company, Inc., Email: muong@burnsmcd.com
(2) Ph.D., P.E., Professor, University of Missouri-Columbia

1. Introduction

One common objective for performing lateral load tests is to establish appropriate p-y models for design of laterally loaded deep foundations. However, the net lateral pressure, p, cannot be directly measured, but rather must be inferred from other measurements via some form of back-calculation to fit some modeled response to the measured response of the deep foundation. This process often requires a number of assumptions regarding the expected structural response of the deep foundation. As illustrated in this paper, such assumptions can have a significant influence of the inferred p-y response.

This paper documents the methodology that was used to develop static p-y curves from experimental measurement results for onshore long flexible drilled shaft, not for the case of cyclic loading or for short rigid pile or for offshore conditions. Background information on the test sites, test instrumentation and test procedure is briefly described. An example of experimental shaft responses in terms of lateral displacements and bending moments along the length of the shaft is presented. Computational program using finite element method developed by the author is used to interpret and derive new p-y curves from the load tests and from the experimental measurement results. Two different methodologies of bending stiffness have been used to verify the reasonable procedure when considering cracking and non-cracking concrete sections. Finally, conclusions drawn from development and evaluation of the proposed procedures and recommendations for implementation and for future work are provided.

2. Lateral Loaded Testing

2.1. Testing Site and Testing Instrumentation

Twenty-five drilled shafts were constructed in Warrensburg and Frankford, Missouri, with diameters ranging from 3 to 5 ft (0.9 to 1.5m) and lengths ranging from 20 to 50 ft (6 to 15m). Each shaft was instrumented with six levels of vibrating wire strain gages, a ShapeAccelArray (SAA), vibrating wire displacement transducers (LVDTs) and dial gages.

All shafts were instrumented with four strain gages at each of six level (24 gages per shaft). The ShapeAccelArray (SAA) devices were used to measure deflection profiles in lieu of a conventional inclinometer. The displacement transducers were connected between the steel casing of the shaft and the reference beam. Mounting the transducers above one another allowed for interpretation of shaft head rotation and displacement at the ground surface. One dial gage was mounted on each shaft during each test. Like the displacement transducers, the dial gages were mounted between the drilled shaft casing and the reference beam. Dial gage measurements were recorded manually in one-minute intervals during testing.

2.2. Lateral Loaded Testing Procedure

The primary focus of the lateral loaded testing program was to measure the response of the foundations subjected to static lateral loading. All tests were performed by pulling two shafts together, so that two foundations were loaded and monitored simultaneously, producing two sets of shaft test results for one individual lateral load test.
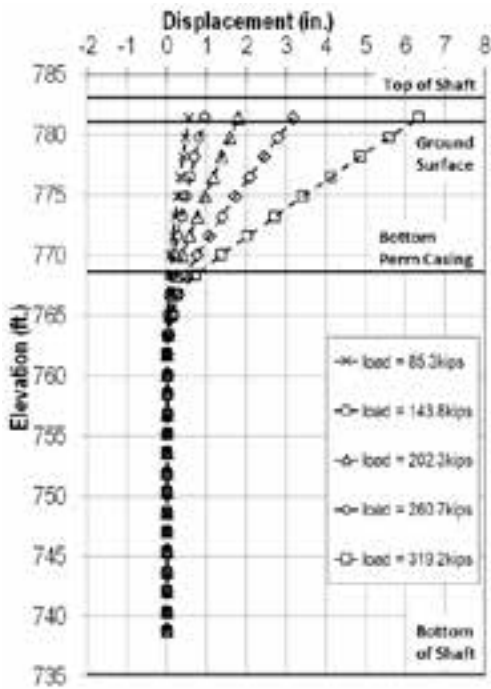
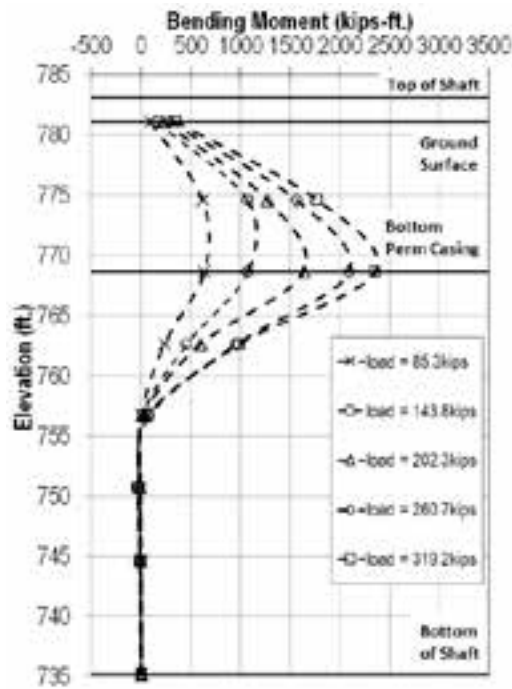Figure 1: Displacement profiles from SAA measurements (shaft W-9)

Figure 2: Bending moment profiles from strain gage measurements (shaft W-9)

In general, the lateral load testing program followed ASTM D3966 (2007). The loads were applied for each test following the loading sequence of Procedure B for Static Excess Loading. Loads were applied using the hydraulic system. For each load test, the load was increased in 200-psi increments, corresponding to approximately 30 kips (133.5 kN) using four jacks. The raw data from strain gages, SAA and LVDTs were recorded continuously with data acquisition devices. Readings from dial gages were recorded every minute.

2.3. Experimental Results

Shaft responses were interpreted from the load test data. The shaft response is characterized by the load-displacement behavior at the top of the shaft, the displacement profiles and the bending moment profiles along the shaft length. Figure 1 represents example of displacement profiles interpreted from SAA measurements. Figure 2 shows example of bending moment profiles obtained using strain gage measurements. Only representative data are presented and discussed in this paper, additional displacement and bending moment profiles are included in Boekmann et al. (2014).

The shapes of the displacement profiles in Figure 1 and the shapes of bending moment profiles in Figure 2 are consistent for all load steps. Increasing of lateral load results in increasing of displacements as well as maximum bending moment. Each displacement profile indicates the respective shaft is essentially fixed around elevation 765, which is 2 to 3 ft (0.6 to 0.9m) below permanent casing.

3. Analysis of Experimental Results

A computational program has been developed using finite element method to analyze drilled shafts subjected to lateral loading. The program derives p-y models to produce the best match of experimental measurements shaft responses for a given shaft geometry and loading.

3.1. Methodology to derive p-y curve models

The program employs the conventional p-y models (Reese et al., 2006; Isenhower and Wang, 2011) to predict the response of a drilled shaft subjected to lateral loading. The p-y model can be implemented through the finite element method (FEM), with the shaft modeled with elastic beam elements and the soil modeled as a series of nonlinear springs. Each spring is governed by a p-y curve, where p is the soil resistance on a unit length of the shaft (force/length) and y is the relative lateral deflection between the soil and the shaft (length).

The shaft responses are governed by:

$$([K_p] + [K_s])\{y_p\} = \{F\} \qquad (1)$$

in which the code solves using the finite element method to produce shaft deflections and rotations.

In Equation 1:

$[K_p]$ = soil stiffness matrix represented by p-y model

$[K_s]$ = stiffness matrix for all the beam elements forming the drilled shaft

$\{y_p\}$ = vector of shaft deflections and rotations at the shaft nodes

$\{F\}$ = vector of induced lateral forces acting on the shaft

The bending moments are then calculated based on the following equation:

$$\{M\} = [EI] \times \{\kappa\} \qquad (2)$$

In Equation 2, bending moments, M, is derived from bending stiffness, EI, and curvature, κ. Finite element method implemented in the program uses shape functions, nodal deflections and nodal rotations to calculate the curvature.

The program applies a p-multiplier to the assumed conventional p-y curve in order to match the experimental measurement shaft responses. The p-multiplier simply factors the values of p on the p-y curves. The program is capable
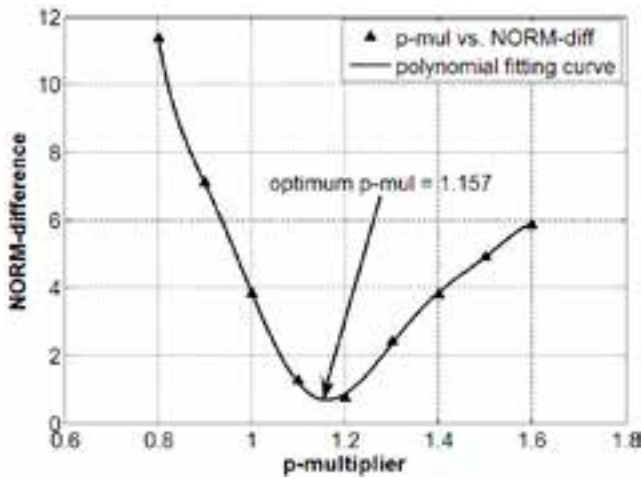
Figure 3: p-multiplier optimization (shaft W-9, load = 319.2kips or 1,420kN)

of matching predicted shaft responses with experimental results, which are displacement profiles from SAA or bending moments from the strain gages. The matching process is outlined in the steps below:

1. A range of p-multiplier values is an input for the program.

2. For each value of the p-multiplier, calculate the difference between the measured and predicted shaft responses values for each node and store the values in a vector. Calculate the norm of each difference vector.

3. Plot the norm of the difference vector versus the p-multiplier as shown in Figure 3. The example would output an optimum p-multiplier value between 1.1 and 1.2.

4. If the curve does not have a minimum, adjust the range of p-multiplier values and repeat steps 2 and 3.

5. Fit a high-order polynomial through the norm versus p-multiplier scatter points. It is called the polynomial fitting curve as shown in Figure 3.

6. The value of the p-multiplier that minimizes the norm corresponds to the best fit of the measured data and will be the optimum p-multiplier.

In Figure 4, several shaft responses in term of lateral displacement and bending moment profiles have been presented for different values of p-multiplier. For a given shaft configuration and at a given load, the optimum p-multiplier obtained from the process above shows the best match between the predicted shaft responses and the experimental measurements.

The methodology of the computational program to establish p-y models starts with adjusting the conventional p-y curves using values of p-multiplier (p-mul) to produce the best fit of experimental measurement shaft responses. After having the optimum p-multiplier, the back-calculation process has been operated to perform the final structural responses in terms of lateral deflections and bending moments. Under a given load and at a given depth, a value of lateral deflection, y, is relative to the lateral soil resistance, p. From series of applied loads, the new p-y model for that given depth will be derived.

The example shown in Figure 5 is performed with shaft W-9, for series of applied loads starting from 26.8kips (120kN) to 348.5kips (1,550kN) and at depth is equal to 2ft (0.6m). For each given load, value of optimum p-multiplier is presented, and each data point represents value of lateral deflection between the soil and the shaft, y, and the corresponding soil resistance on a unit length of the shaft, p.
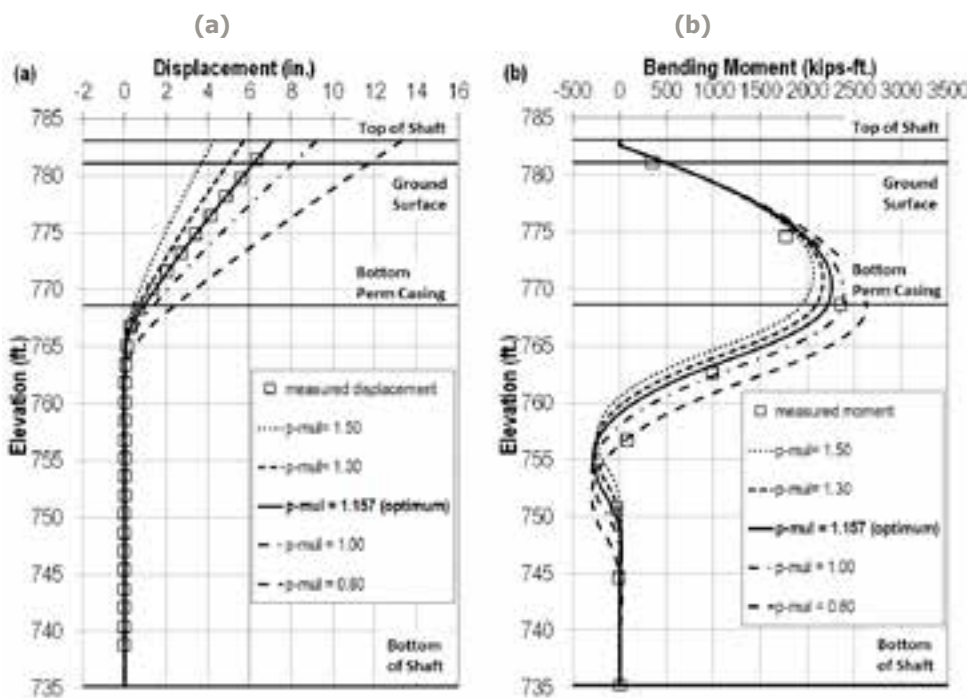
Figure 4: Shaft responses for different values of p-multiplier (shaft W-9, load = 319.2kips or 1,420kN)

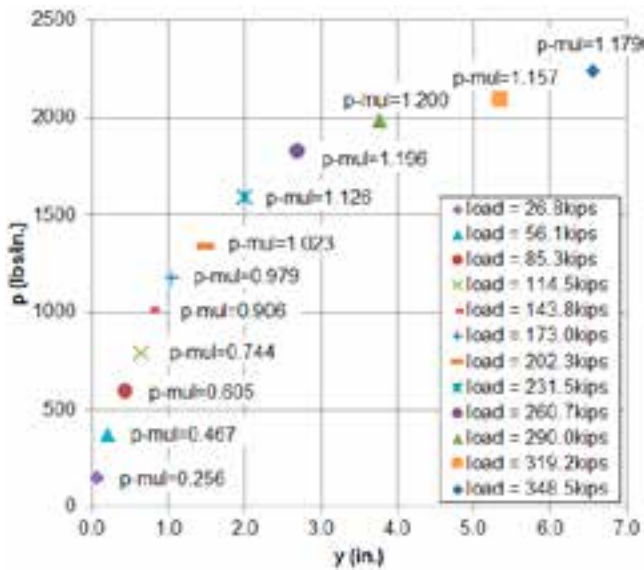(a) Displacement   (b) Bending Moment

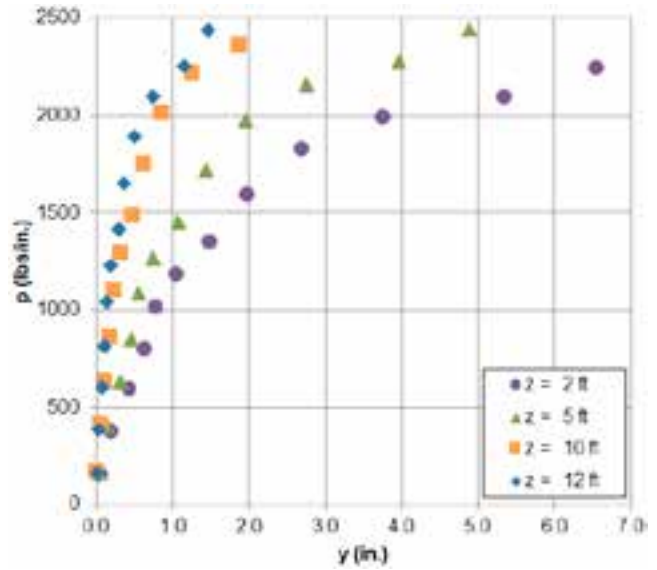**Figure 5: Predicted p-y curve derived from the experimental results (shaft W-9, depth z=2ft or 0.6m)**

Figure 6: Different predicted p-y curves derived from the experimental results for different depths (shaft W-9, z=2ft (0.6m), 5ft (1.5m), 10ft (3m), 12ft (3.6m))

Different predicted p-y models for the same shaft but at different depths can be derived easily since the optimum p-multiplier and the shaft responses are unchanged. The lateral deflection, y, for a different depth need to be obtained from the shaft responses and new value of lateral soil resistance, p, is calculated. Repeat the procedure for all the applied loads to derive the predicted p-y models for different depths.

Figure 6 shows different predicted p-y curves for the same shaft W-9 at four different depths of 2ft, 5ft, 10ft and 12ft (0.6m, 1,5m, 3m and 3.6m).

3.2. Methodologies for bending stiffness

The bending stiffness, EI, is nonlinear and greatly influenced by concrete cracking, which is difficult to predict. Two methodologies of using bending stiffness have been presented to illustrate the reasonable procedure implementation in the computational program to derive the p-y models.

The first methodology of bending stiffness simply considers the cross-section geometry and material properties of the drilled shaft. Assume that no cracking of concrete is given during the lateral loaded test, the bending stiffness will be linear along both casing and non-casing sections as shown in Figure 7.

The second methodology of bending stiffness considers the nonlinear properties due to the cracking of concrete sections. The routine employed by LPile is documented in the program's technical manual (Isenhower & Wang, 2011). In summary, LPile iterates the location of the neutral axis until force equilibrium is satisfied, accounting for concrete cracking. Cracking of the concrete is predicted as a function of the compressive strength of the concrete, which was estimated from compression tests performed on cylinders from each shaft pour.

An example of the nonlinear shaft bending stiffness predicted by LPile as a function of the bending curvature is shown in Figure 7. The nonlinear bending stiffness decreases abruptly at small values of curvature, which initiate cracking of the concrete. After the concrete cracks, the decrease in stiffness is more gradual as the steel yields.

The procedure used here predicted values of bending stiffness along the length of the shaft as a function of the bending curvature, which was interpreted from computational program using initial assumed value of bending curvature. Predicted values for bending stiffness as a function of curvature were computed using Ensoft LPile. These values were used to implement in the computational program, especially in the iteration process presented below:

1. An initial bending stiffness is assigned to each element of the shaft.

2. Calculate the bending curvature from the deflection derived from that initial EI.

3. Obtain improved values of bending stiffness EI using the calculated bending curvatures from Step 2 and the predicted EI curves as shown in Figure 7.
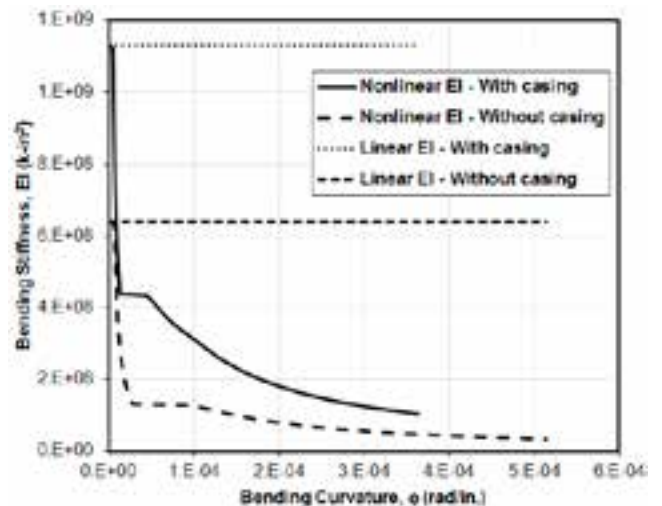

Figure 7: Example of linear and nonlinear bending stiffness for shaft W9

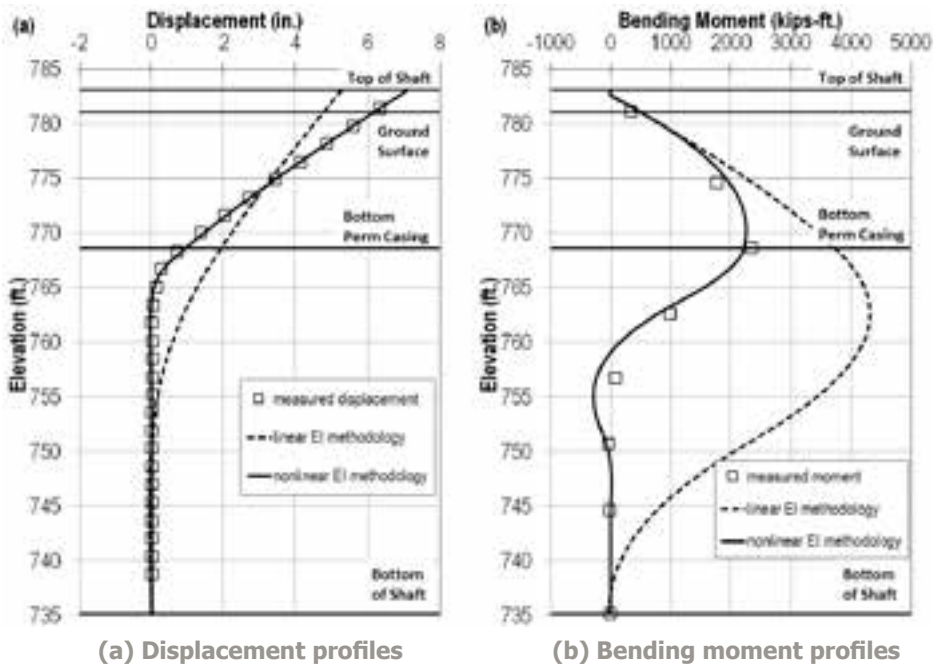(a) Displacement profiles   (b) Bending moment profiles

Figure 8: Predicted and measured shaft responses (shaft W-9, load = 319.2kips or 1,420kN)

4. Repeat steps 2 and 3 until the approximate relative error in EI values is negligible.

4. Predicted Responses

The analyses of experimental measurements explained in the previous section were applied to all 25 test shafts to produce predicted displacement, bending moment and p-y models considering linear and nonlinear EI. Example results are presented and discussed below.

4.1. Predicted lateral deflections

Figure 8a shows the difference between predicted lateral deflections using two different methodologies of bending stiffness: linear and non-linear. The measured lateral deflection obtained from SAA measurements has been presented also in order to compare with the predicted ones.

The shapes of the predicted displacement profiles indicate that by using nonlinear bending moment methodology, the predicted displacements are closely fit with the measured ones. While the linear bending stiffness methodology shows the substantial differences between predicted and measured ones.

Predicted displacement profiles obtained using nonlinear bending moment methodology show that the respective shaft is essentially fixed around the elevation 765 below the top
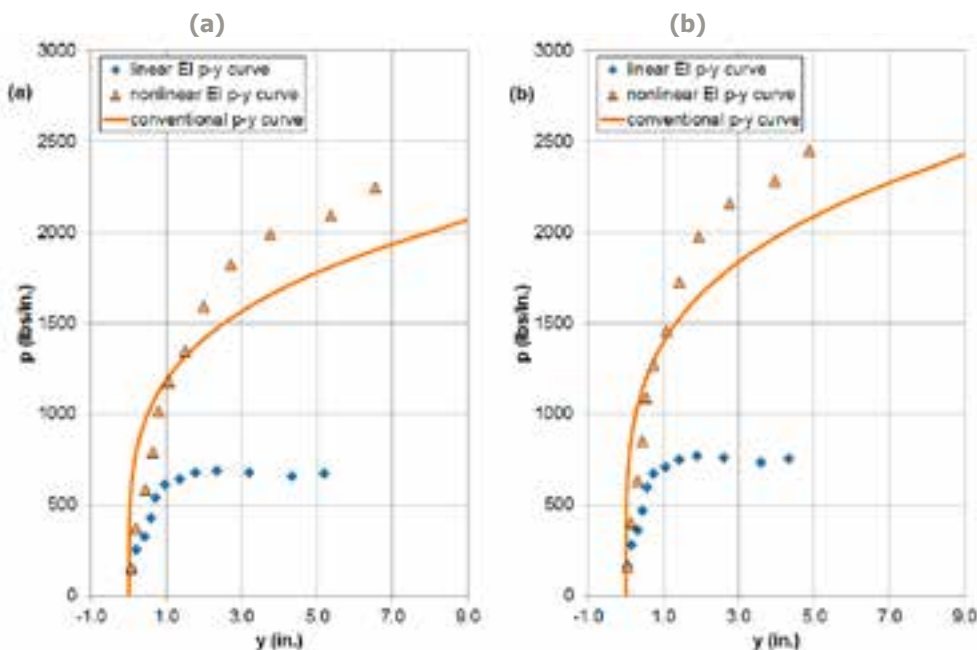

Figure 9: Predicted p-y curves using different stiffness methodologies vs. conventional p-y curve at: (a) depth = 2ft or 0.6m ; (b) depth = 5ft or 1.5m
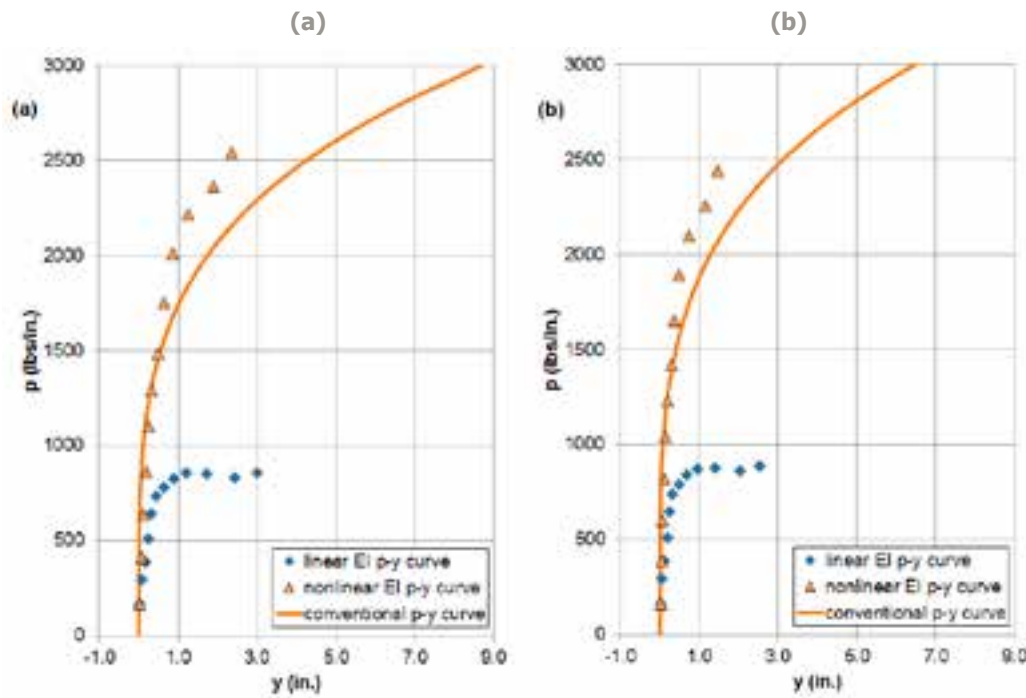
(a)   (b)

Figure 10: Predicted p-y curves using different bending stiffness methodologies vs. conventional p-y curve at:

(a) depth = 10ft or 3m   **(b) depth = 12ft or 3.6m**

of the shaft, which is the same as the shaft responses fixed elevation obtained from experimental measurements.

4.2. Predicted bending moments

Figure 8b shows values of the bending moment interpreted from the strain gage measurements as well as values predicted by the computational program using linear and nonlinear bending stiffness methodologies.

The predicted bending moments using the methodology of nonlinear bending stiffness show a reasonably good fit to the bending moments interpreted from the strain gage measurements. While the linear bending stiffness methodology shows many differences between predicted and measured displacements. Reason is the much higher values of linear bending stiffness results in higher values of bending moments

4.3. Predicted p-y curves

Figure 9 and Figure 10 shows the difference between predicted p-y curves at a given depth using two different methodologies of bending stiffness: linear and non-linear. The conventional p-y curves (Reese et al., 2006; Isenhower and Wang, 2011) have been presented to compare with the predicted ones.

There is a significant difference between the predicted p-y curves using two different methodologies of bending stiffness as shown in Figure 9 and Figure 10. The predicted p-y curve using nonlinear bending stiffness methodology has much higher ultimate value of lateral response since the nonlinear bending stiffness reasonably represents the actual stiffness of the shaft, especially when the concrete is cracked.

The predicted p-y curves derived from experimental measurements are compared to the conventional p-y curves for stiff clay model (Reese et al., 2006; Isenhower and Wang, 2011). Interpretation of data from Figure 9 and Figure 10 indicate close agreement between the predicted p-y curves

using nonlinear bending stiffness methodology and the conventional p-y curves.

The initial slopes are similar for predicted p-y curves using nonlinear bending stiffness and conventional p-y models, while predicted p-y curves using linear bending stiffness methodology have much lower initial slopes.

Data generally indicates slightly greater values of ultimate lateral soil responses for nonlinear bending moment methodology but much lower values for linear bending stiffness methodology, compared with the conventional p-y curves values.

As the depths increase in Figure 9a, 9b, 10a and 10b, the initial slopes as well as the ultimate lateral soil responses of predicted p-y curves increase, which shares the same characteristic with the conventional p-y curves.

5. Conclusion

Shaft responses in terms of lateral deflection and bending moment profiles were interpreted from strain gages and shape acceleration array (SAA) measurements. A methodology of matching predicted and collected data has been established and implemented in the computational program using Finite Element Method in order to generate experimental p-y response from measurements of displacement and strain. Moreover, in the case when bending stiffness (EI) is nonlinear and greatly influenced by concrete cracking, the importance of using nonlinear bending stiffness is represented by comparing the difference of shaft responses as well as predicted p-y curves using two different methodologies of bending stiffness. Among the most important observations:

- The computational program using Finite Element Method written to fit p-y model parameters by using p-multiplier to the experimental measurements obtained from geotechnical instrumentations was similarly effective.

rockfall source in a realistic manner.

However, HoloLens 2 itself has the following problems:

(1) Since the device itself does not have position information like GPS, it is not easy to align the BIM/CIM model of slopes with the position in real space.

(2) It takes time to load the 3D data with a large file size to display the hologram with HoloLens 2.

(3) The device itself is not dust-proof or drip-proof, and the system is likely to go down under conditions where the temperature is 30° C or higher.

Regarding the solutions for the above-stated issues, for (1), it is possible to perform accurate alignment by combining it with the position correction technology of the quasi-zenith satellite "MICHIBIKI" [7], which is operated by JAXA [8]. Regarding (2), the 3D model should be optimized to reduce the size as much as possible before being displayed with HoloLens 2. For the issue stated in (3), we expect that next-generation devices developed in the future can withstand use under harsh conditions such as in the civil engineering and construction site. Some cooling equipment for HoloLens 2 was also introduced and we hope that these accessories will be developed further to help HoloLens 2 work better in multiple types of environments./.

References

1. Microsoft Corporation 2022, digital image, accessed 2022 Feb 14th, <https://docs.microsoft.com/en-us/windows/mixed-reality/design/core-concepts-landingpage>.

2. Autodesk Inc. Architecture, Engineering & Construction Collection, accessed 2022 May 19th, <https://www.autodesk.com/collections/architecture-engineering-construction/overview?term=1-YEAR&tab=subscription >.

3. ITOCHU Techno-Solutions Corporation. Solution and Products, accessed 2022 May 19th, <https://www.engineering-eye.com/en/category/45/index.html>.

4. Robert McNeel & Associates. Rhinoceros 3D, accessed 2022 May 19th, < https://www.rhino3d.com/en/>.

5. Fologram Pty Ltd. "Fologram for Rhino and Grasshopper" and "Fologram for HoloLens", accessed 2022 May 19th, <https://fologram.com/download >.

6. K. Miura, N. Komuro, N. Kuramoto. Extraction of rock-fall danger points related to road disaster prevention using laser profiler data. Journal of JGS, Vol.69□No.6□30-33, 2021. (Japanese)

7. Construction IT World. Quasi-zenith satellite "MICHIBIKI", HoloLens2, BIM / CIM are linked. Challenge to construction management of construction site by MR (Informatics), accessed 2022 Jan 17th, <https://ken-it.world/success/2021/03/michibiki-mr-collaboration.html#>.

8. Japan Aerospace Exploration Agency. Overview of the First Quasi-Zenith Satellite "MICHIBIKI", accessed 2022 April 14th, <https://global.jaxa.jp/countdown/f18/overview/michibiki_e.html>.

Development of static P-Y curves from experimental measurements...

- Optimization p-multiplier process produces closed fit between the predicted shafts responses and the collected measurements.

- Nonlinear characteristic of bending stiffness is important and significantly impacts the predicted shaft responses in terms of lateral displacements and bending moments, as well as the predicted p-y models.

- Linear and nonlinear methodologies of applying bending stiffness to the computational program show the substantial differences in both shapes and magnitudes of predicted shaft responses and the significant differences of predicted p-y models.

- By using nonlinear bending stiffness considered the cracking of concrete section and the methodology to derive p-y models implemented in the computational program, the experimental p-y curves can be established reasonably and practicably.

- The p-y curves derived from experimental measurements are compared to the conventional p-y curves. The comparisons are useful for perspective on how the test data align with models commonly assumed in practice.

The proposed approach is limited to the static p-y curves for onshore long flexible drilled shafts, not for the case of cyclic loading or for short rigid pile or for offshore conditions. Further readings should refer to API RP 2A-WSD, 22nd Edition, November 2014 and DNVGL-RP-C212, 2019 Edition, September 2019./.

References

1. ASTM Standard D3966. Standard Test Methods for Deep Foundations Under Lateral Load. ASTM International, West Conshohocken, PA, 2007, DOI: 10.1520/D3966-07, www.astm.org, 2007.

2. Boeckmann, A.Z., Myers, S.G., Uong, M. and Loehr, J.E. Load and Resistance Factor Design of Drilled Shafts in Shale for Lateral Loading. Report to Missouri Department of Transportation, 2014.

3. Isenhower, W.M. and Wang, S.-T. Technical Manual for L-Pile, Ensoft, Inc., Version 6, 2011.

4. Reese, L.C., Isenhower, W.M. and Wang, S.-T. Analysis and Design of Shallow and Deep Foundations, John Wiley & Sons, Hoboken, New Jersey, 2006.